Soil Dynamics and Earthquake Engineering 175 (2023) 108228

Contents lists available at ScienceDirect

Soil Dynamics and Earthquake Engineering

journal homepage: www.elsevier.com/locate/soildyn

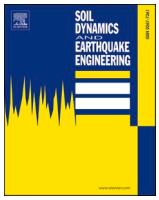

Vertical seismic ground shaking in the volcanic areas of Italy: prediction equations and PSHA examples

Fadel Ramadan, Giovanni Lanzano *, Sara Sgobba

Istituto Nazionale di Geofisica e Vulcanologia, Italy

ARTICLE INFO

Keywords:
Ground motion models
Volcanic earthquakes
Vertical component
Italy
Seismic hazard

ABSTRACT

This work introduces a new Ground Motion Model (GMM) to predict the horizontal and vertical components of PGA, PGV and acceleration response spectra up to 5s for the volcanic events in Italy. The model updates the GMM for the horizontal components, recently developed by Lanzano & Luzi [1], and shows relevant amplitudes in near-source and a frequency content richer in intermediate-to-low frequencies. The comparison with an event not used for the calibration and belonging to another volcanic district in Italy is promising for the extension of the model to other areas. Finally, we present a case study of a site, in the proximity of Mount Etna in eastern Sicily region, which allows us to evaluate the impact of these models in the framework of a Probabilistic Seismic Hazard Analysis (PSHA).

1. Introduction

The earthquakes caused by volcano activities occur as a consequence of the magma movement and gases migration from depth to Earth surface. In Italy, where the active volcanoes are in heavily populated areas (e.g., the city of Catania, the Ischia Island, the Phlegrean fields, the Mount Vesuvius, and surroundings), these types of earthquakes demonstrated to have similar damaging impacts as those occurring in shallow active crustal regions, as reported from the macroseismic observations of historical earthquakes (DBMI v. 4.0 [1,2]). During the July 28, 1883 (M_W 4.6) volcanic earthquake on the Ischia Island (https://emidius.mi.ingv.it/CPTI15-DBMI15/event/18830728_2025_000), a macroseismic intensity of 10 was assigned to the locality of Casamicciola Terme, because of the severe damage or collapse of several buildings.

Several authors [3,4] recognized two types of earthquakes induced by volcanic activities: i) Long-period (LP) earthquakes, caused by cracks resonating as magma and gases move toward the surface; ii) Volcano-tectonic (VT) earthquakes that represent a brittle failure of rock, a process similar to that occurring along purely "tectonic" faults. The LP earthquakes have some peculiar features, such as [3], i) a "burst" of high frequencies at short distances, ii) a long monotonic coda and iii) velocity spectra with a dominant and sharp peak in the range 1–2 Hz. On the contrary, VT earthquakes have characteristics more similar to earthquake that occurred in shallow active crustal regions. Based on the observations of the ground motion at Mount Etna, Tusa and Langer [4] approximately recognized the threshold depth of 5 km to separate the LP and VT events. These observations are also confirmed by tomographic studies of the main volcanic edifices in Italy, i.e., Mount Etna [5], the Phlegrean fields [6] and the island of Ischia [7], which show that most of the LP seismicity is concentrated in the shallower upper crust.

As an additional feature, from the analysis of the macroseismic observation [8] and the available recordings, the attenuation with distance is found to be generally faster than the shallow crustal earthquakes. Finally, because of the high frequency "burst" of LP events, the peak parameters are remarkably high very close to the event source [9]. If the event is very shallow, these features may be particularly relevant from an engineering design and must be considered in seismic hazard estimates [10,11].

More recently, several efforts were made to derive empirical equations to predict the strong ground motion produced by volcanic earthquakes. One of the first in Italy was derived by Tusa and Langer [4] for the events of Mount Etna region. In this study, the Authors used two different predictive equations for earthquakes with focal depth <5 km (shallow) and >5 km (deep). The shallow events GMM was then revised by Peruzza et al. [10], with the introduction of the hypocentral distance, as an explanatory variable.

As a consequence of the Mount Etna (mainshock December 26, 2018 Mw = 4.9) and Ischia Island (mainshock August 21, 2017 Mw = 3.9) earthquakes, the number of recordings of engineering interest remarkably increased, because these events are very shallow and have been

* Corresponding author.
E-mail addresses: fadel.ramadan@ingv.it (F. Ramadan), giovanni.lanzano@ingv.it (G. Lanzano), sara.sgobba@ingv.it (S. Sgobba).

https://doi.org/10.1016/j.soildyn.2023.108228
Received 21 April 2023; Received in revised form 31 July 2023; Accepted 2 September 2023
Available online 14 September 2023

recorded by stations very close to the epicenter. Lanzano and Luzi [1] took advantage of the new observations to calibrate a new predictive model for the horizontal component of PGA, PGV and the ordinates of the 5%-damped acceleration response spectra (SA) in the period range T = 0.025–5s. The novel model extended the validity pre-existing models by increasing the maximum magnitude to 4.9 and was able to overcome the limitations of previous models by showing a remarkable ability to predict seismic motion in near source. Later, Tusa et al. [12] updated the previous 2016 model, taking advantage of the near-source records of the 2018 sequence at Mount Etna. The Authors introduced in the functional form a magnitude-dependent pseudo-depth according to the scaling by Azzaro et al. [13], improving the model in terms of total error.

The above-listed models have been developed only for the horizontal component of the seismic motion, mainly because seismic design actions are commonly provided in terms of horizontal ground motion components, in the form of a design response spectrum. As a result, there are currently no models that predict the vertical component for volcanic earthquakes in Italy, even though this component has been shown to be relevant for engineering design [14]. As a matter of fact, the vertical component of tectonic earthquakes was found to be larger than horizontal one close to the causative source, especially at short periods. Some examples are provided by Ramadan et al. [14] for shallow active crustal events, during the recent Italian sequences of 2012 Po plain and 2016–2017 Central Italy.

To overcome this gap in ground motion modelling and evaluate the implications on seismic design for vertical seismic actions of structures in volcanic areas, the main objective of this paper is to analyze the vertical ground motion and update the model developed by Lanzano and Luzi [1], to predict both the horizontal and vertical components of PGA, PGV and the acceleration response spectra for the volcanic earthquakes in Italy.

2. LL19 update

The dataset for the model calibration is the same as LL19 and collects waveforms of events that occurred in some of the volcanic zones of Italy, namely the Mount Etna, the Aeolian Islands, and the island of Ischia (Fig. 1). The strong-motion parameters have been computed from the waveforms available at the Engineering Strong-Motion database (ESM, https://esm-db.eu [15]) and the Italian Accelerometric Archive (ITACA, https://itaca.mi.ingv.it [16]). The networks and the corresponding providers are: i) Rete Accelerometrica Nazionale [RAN], code IT [17] managed by the Italian Department of Civil Protection; ii) Italian National Seismic Network [INSN], code IV [18], managed by the Istituto Nazionale di Geofisica e Vulcanologia (INGV); iii) network MN (Mediterranean Network [MEDNET] project, code MN [19]), also managed by INGV. Since some IV stations are equipped with co-located accelerometric and broadband instruments and, generally, both records are available for each event, we prefer to keep in the dataset only the broadband records, in order to avoid oversampling. All the waveforms were uniformly processed using the strong-motion processing tool the Engineering Strong Motion database (ESM, https://esm-db.eu/processing/select; Puglia et al. [20]), following to the scheme proposed by Paolucci et al. [21].

The final set is composed of 615 records of 41 events, occurring in the time span 2001–2019, recorded by 155 stations. The event metadata was revised according to the procedure described in Lanzano and Luzi [1], resulting in a magnitude range of 3.0–4.9. The shear wave velocity V_S profiles with depth are available only for about 13% of the stations, allowing to compute the average velocity in the uppermost 30 m, $V_{S,30}$, according to the EC8 [22]; in the remaining cases, $V_{S,30}$ is computed from correlation with the topographic slope [23].

The dataset includes some recordings with vertical peak ground acceleration PGA_v>0.1 g in near source conditions (epicentral distances lower than 5 km), i.e., the record of IV station Casamicciola (station code IOCA) during the Ischia earthquake (August 21, 2017 M_W 3.9) with vertical PGA_v = 0.27 g (R_{epi} = 0.9 km), and the record of the IT station Santa Venerina (station code SVN) during the Viagrande (Etna) earthquake (December 26, 2018 M_W 4.9) with vertical PGA_v = 0.15 g (R_{epi} = 4.5 km). In particular, the ratio between the vertical component of the PGA and the maximum horizontal component is about 1 in the first case (IOCA) and becomes greater than unity for the low period ordinates of the acceleration response spectrum (about 1.5 at vibration period 0.3s).

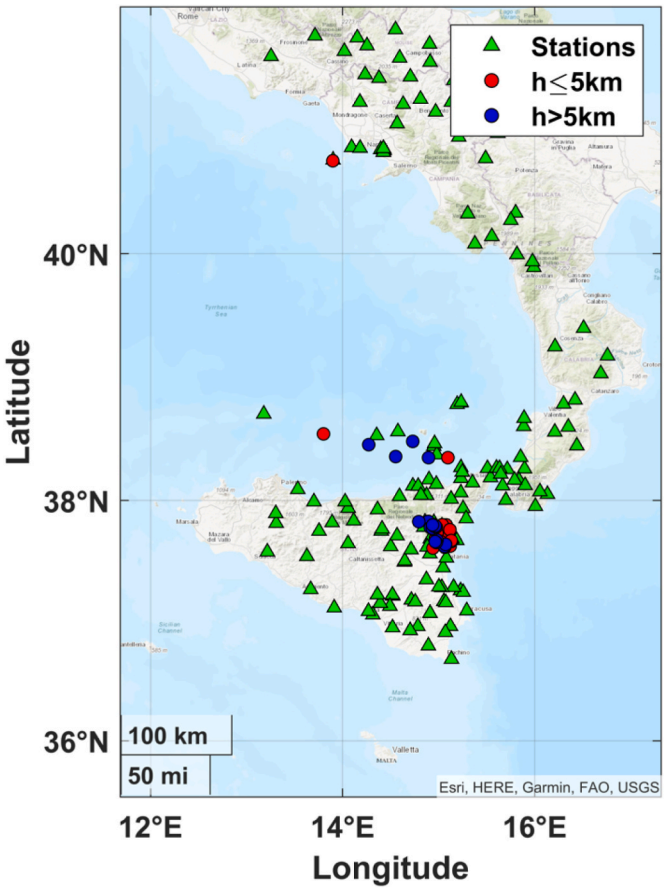

Fig. 1. Location of the events and stations in the dataset for model calibration; h is the focal depth of the events.

As observed by several authors [1,4], volcanic earthquakes show different characteristics with respect to events of tectonic origin, especially if they are very shallow. Fig. 2 reports the vertical-to-horizontal ratios data points as a function of hypocentral distance, in the cases of deep or shallow events: no trend is observed for short and long periods, shallow and deep events, indicating that the scaling with the distance for the vertical and horizontal component is the same. In particular, (see Figure 1 of Electronic Supplement S1), the short period vertical component amplitudes of the deeper events show less rapid attenuation and signs of anelastic attenuation, while shallow events show faster attenuation and negligible anelastic attenuation. A magnitude-dependent attenuation of ground motion, which is usually visible for magnitudes greater than 5, is not clearly observed. Similar considerations can be carried out concerning the attenuation with distance at long periods, although the differences between surface and deep earthquakes are smaller.

In addition, Fig. 2 show that vertical-to-horizontal ratio is lower than 1 in most of the cases, even in near-source conditions, where the SA-T = 1s amplitudes are remarkably lower than unity. As mentioned above, the exception is the IOCA recording of the Ischia earthquake, which shows a ratio of slightly more than one at short periods.

Since the dependencies on the explanatory variables are very similar to those observed by Lanzano and Luzi [1] for the horizontal

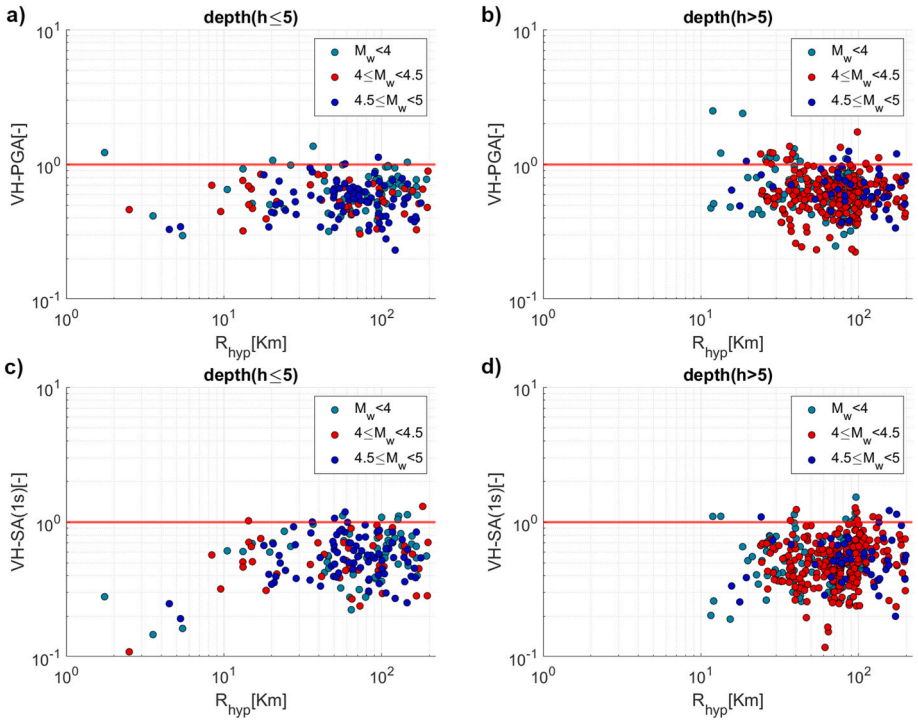

Fig. 2. Vertical-to-horizontal ratios vs. hypocentral distance for different classes of magnitude: a) PGA and shallow earthquakes (h ≤ 5 km); b) PGA and deep earthquakes (h > 5 km); c) SA at T = 1s and shallow earthquakes; d) SA at T = 1s and deep earthquakes.

components (linear magnitude scaling, different geometrical attenuation for shallow and deep events and the effect of anelastic attenuation only for deep events), we assume the same functional form for both the horizontal and vertical model for the calibration of the predictive equations, which is:

$$log_{10}\, Y = a + bM_W + F_D(R, M_W) + F_S + \delta B_e + \delta S2S_S + \delta WS_{es} \quad [1]$$

a is the model offset and M_W is the moment magnitude. If M_W is not available, we alternatively use the local magnitude M_l, without any conversion. However, we checked that the use of the magnitude conversion equations, such as the model by Gasperini et al. [24], has no effect on the median prediction and variability of the model, while it even results in a small increase in the total standard deviation. Indeed, the dataset consists mostly of low magnitude earthquakes for which the differences between the two metrics are limited.

The term distance $F_D(R)$ is updated with respect to the original LL19 model, by introducing a magnitude dependent geometric attenuation, as:

$$F_D = \begin{cases} c_1\, log_{10}\sqrt{R_{hyp}{}^2 + h_1{}^2} + c_2\left(M_w - M_{ref}\right) log_{10}\sqrt{R_{hyp}{}^2 + h_1{}^2} & focal\ depth\ h \le 5km \\ c_3\, log_{10}\sqrt{R_{hyp}{}^2 + h_2{}^2} + c_4\left(M_w - M_{ref}\right) log_{10}\sqrt{R_{hyp}{}^2 + h_2{}^2} + c_5\sqrt{R_{hyp}{}^2 + h_2{}^2} & focal\ depth\ h \le 5km \end{cases} \quad [2]$$

where R_{hyp} is the hypocentral distance and M_{ref} is the reference magnitude, which was set at 4.8, regardless of the ground motion intensity measure, based on preliminary nonlinear calibrations of the SA coefficients at short periods, where the magnitude dependent geometric attenuation is more apparent (see Figure 2 of Electronic Supplement S1). Two different pseudo-depths are adopted for surface (h_1 = 1 km) and deep (h_2 = 5 km) events.

The site term is introduced as a dummy variable ($F_S = s_i$ with i = 1,2,3) according to the subsoil classes of EC8, where i = 1 corresponds to rock sites of class A ($s_1 = 0$), i = 2 to stiff soils (class B) and i = 3 to soft soils of class C and D.

The functional form in Eq [1]. also includes the random terms related to event (between-event, δB_e) and site (site-to-site, $\delta S2S_s$), and the leftover aleatory residual (event- and site-corrected, δWS_{es}), following the partially non-ergodic ground motion modeling scheme [25]. The linear mixed-effect model [26] was used to calibrate the fixed coefficients (a, b, c_1, c_2, c_3, $s_1 = 0$, s_2 and s_3) and the random terms (δB_e and $\delta S2S_s$): each random term is log-normally distributed with zero-mean and standard deviations τ for δB_e and φ_{S2S} for $\delta S2S_s$, respectively. The standard deviation of δWS_{es} is σ_0 and the total standard deviation σ is computed as:

$$\sigma = \sqrt{\tau^2 + \varphi_{S2S}^2 + \sigma_0^2} \quad [3]$$

Like the LL19, the proposed model is calibrated for PGA (cm/s^2), PGV (cm/s) and 30 ordinates of SA (from T = 0.025s to T = 5s). The coefficients of the regression and the associated standard deviation for the horizontal and vertical components are reported in electronic appendices (Supplement S2). The residuals (between-event, site-to-site, and site- and event-corrected residuals) as a function of the explanatory variables (moment magnitude, site class, and hypocentral distance, respectively) do not present relevant bias, as shown in the plots of the electronic supplement for PGA and SA(1s) (see Figure 3 of Electronic Supplement S1).

Other plots are available in the supplement showing the comparison

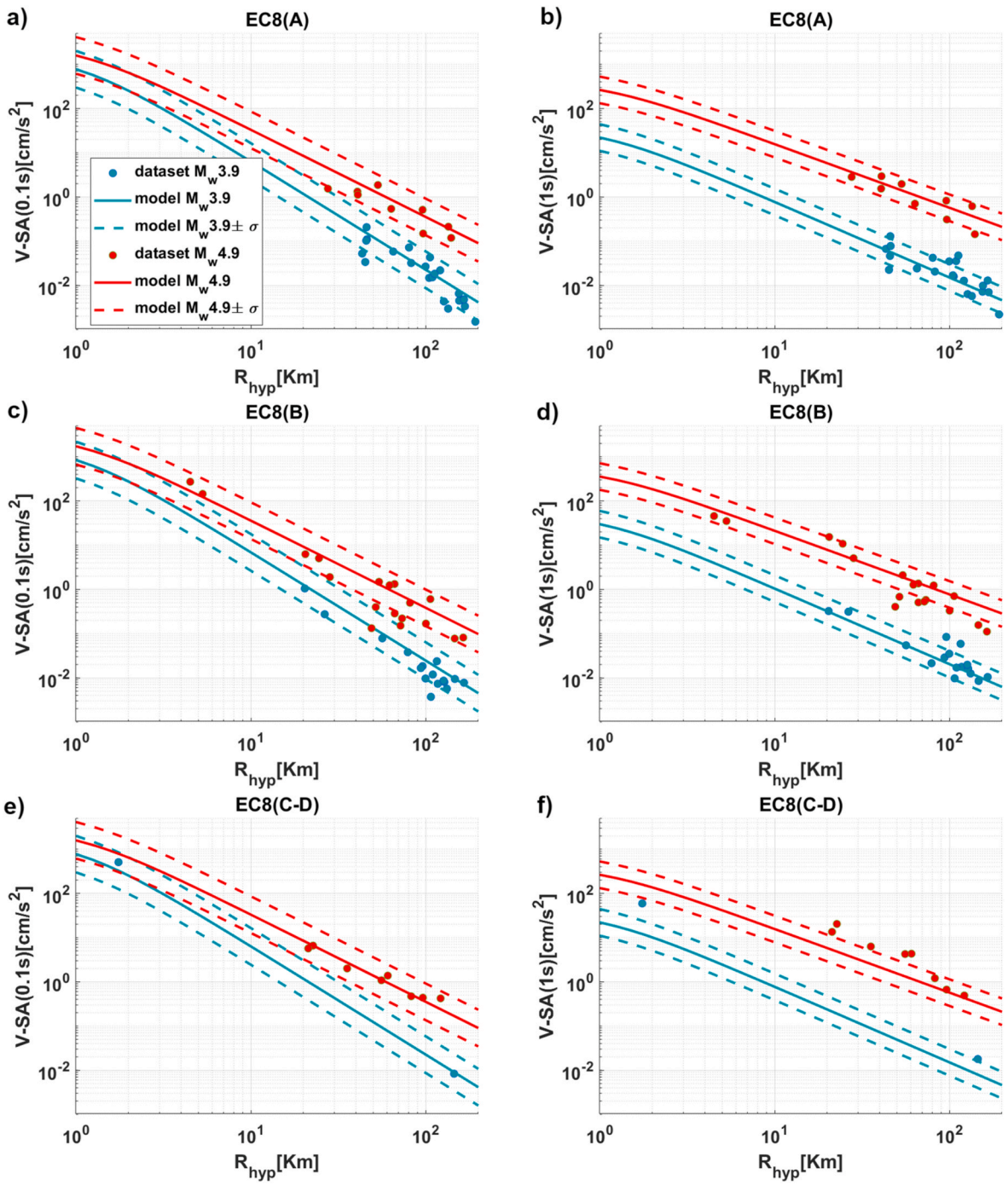

Fig. 3. Comparison between median predictions (±σ) and observations for the vertical component of PGA (left) and SA(1s) (right) as a function of R_{hyp}, for M_w 3.9 and M_w 4.9 for soil type A (top), soil type B (middle) and soil type C-D (bottom).

between the model of Eq [1]. for the horizontal components and LL19, both in terms of median prediction and variability (see Figures 4–6 of Electronic Supplement S1): the introduction of the magnitude-dependent geometric attenuation term allows better capturing of the trend with distance of lower magnitude earthquakes; in addition, the τ shows an average reduction of 12%, which is reflected in a reduction of the total variability σ by 10%.

3. Results

Fig. 3 shows the comparison between the model predictions and the empirical data of two relevant earthquakes in the calibration dataset, i.e., the M_W 3.9 Ischia Island event and the M_W 4.9 Viagrande event. The model proposed here reasonably matches the observations, like the model for horizontal components (see Fig. 4 of Electronic Supplement S1), both for the Viagrande and Ischia earthquakes, also due to the introduction of the magnitude-dependent attenuation term, which allows to better capture the trend with distance for the lower magnitude events. Considering the scenario of $R_{hyp} = 1$ km and EC8-A site category, the PGA predictions of the proposed model are lower than those provided by the model for horizontal components: for $M_W = 3.9$ $PGA_v = 0.08$ g and $PGA_h = 0.1$ g; for $M_W = 4.9$, $PGA_v = 0.4$ g and $PGA_h = 0.7$ g. Similar evidence can be found for the other subsoil categories and for the long periods.

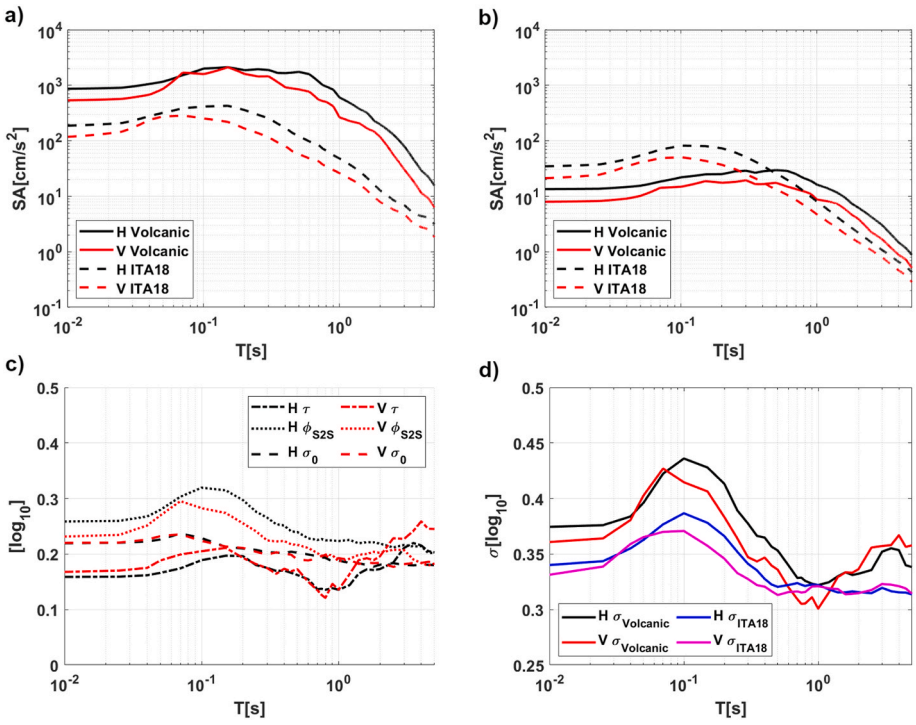

Fig. 4. Comparison among GMMs: predicted spectra for M_W 4.9, $V_{S,30}$ = 800 m/s, h = 1 km and two hypocentral distances: a) R_{hyp} = 1 km and b) R_{hyp} = 15 km; c) non-ergodic components of standard deviation of the volcanic models; d) total standard deviations. H and V volcanic are the GMMs presented here; H ITA18 is the model by Lanzano et al. [27]; V ITA18 is the model by Ramadan et al. [14]. The ITA18 predictions are provided for normal faulting earthquakes.

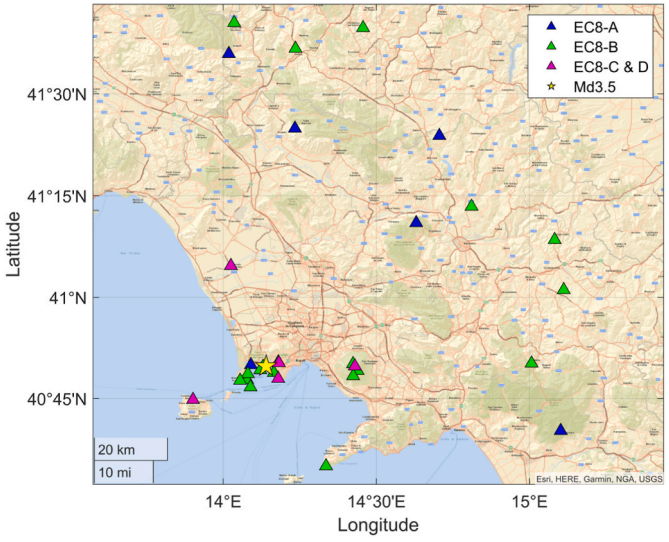

Fig. 5. Map of the Phlegrean fields March 16, 2022, M_d 3.5, earthquake epicenter and the recording stations.

Fig. 4a and b shows the acceleration response spectra for horizontal and vertical components of the predictive models for volcanic and purely tectonic events in Italy. The GMMs for crustal events are the ITA18 [27] for horizontal components and the ITA18 corrected with the V/H scaling factor proposed by Ramadan et al. [14] for the vertical components. Two scenarios are selected (two hypocentral distances R_{hyp} = 1 km and 15 km), both relative to a very shallow earthquake (h < 5 km) and a moderate magnitude (M_W 4.9).

The spectral amplitudes of the volcanic GMMs are higher than those predicted by the crustal model at very short distances; this is the effect of the high frequency "burst", typical of the LP events in near source conditions. Moreover, the peak of the spectra of the volcanic models is shifted to longer periods (T = 0.3s vs 0.1s for tectonic model). At longer distances and short periods, the amplitudes are smaller than the ITA18-like GMMs, while at longer periods the predictions of volcanic models equal and exceed (for T > 1s) the predictions of models for crustal earthquakes. These differences are caused by the faster attenuation of shallow volcanic events with respect to those occurring in active shallow crustal contexts. In all cases, the predictions for the vertical component are lower than those provided by the model for the horizontal, even for crustal earthquakes: This is because vertical amplitudes greater than horizontal amplitudes are generally observed for events with Mw > 4.9 (see Ref. [14]).

Fig. 4c shows the non-ergodic standard deviations of the new models for horizontal and vertical components as a function of the period: the between-event standard deviation τ of the vertical model is quite similar to the horizontal τ at short period, while increase at longer periods (T > 1s); the site-to-site standard deviation φ_{S2S} is the largest variability for both components, but the horizontal φ_{S2S} is on average 9% larger than the vertical one; the event- and site-standard deviations (σ_0) are the same regardless of horizontal and vertical components. As remarked by Lanzano and Luzi [1] concerning the φ_{S2S} large values, "[….] the classification of sites is challenging, due to the large variability in the stiffness of volcanic deposits and rocks and the paucity of geophysical tests". As a matter of fact, several authors [28–31] have shown that the amplifications of the most superficial thicknesses of some volcanic soils might not be best described using only $V_{S,30}$ as a proxy. In fact, many sites are characterized by strong shear wave velocity inversions with depth caused by layers of compact lava flow overlying softer soils: the amplification of these sites is not assimilable to any class of EC8 soil categories, that commonly assumes stratigraphic successions with V_S increasing with depth.

Fig. 4d shows the total standard deviation of the volcanic and tectonic models: the standard deviations of volcanic GMMs are in the range 0.3–0.45 log10 units and is generally higher than the ones obtained for active crustal regions. This larger variability could be related to the

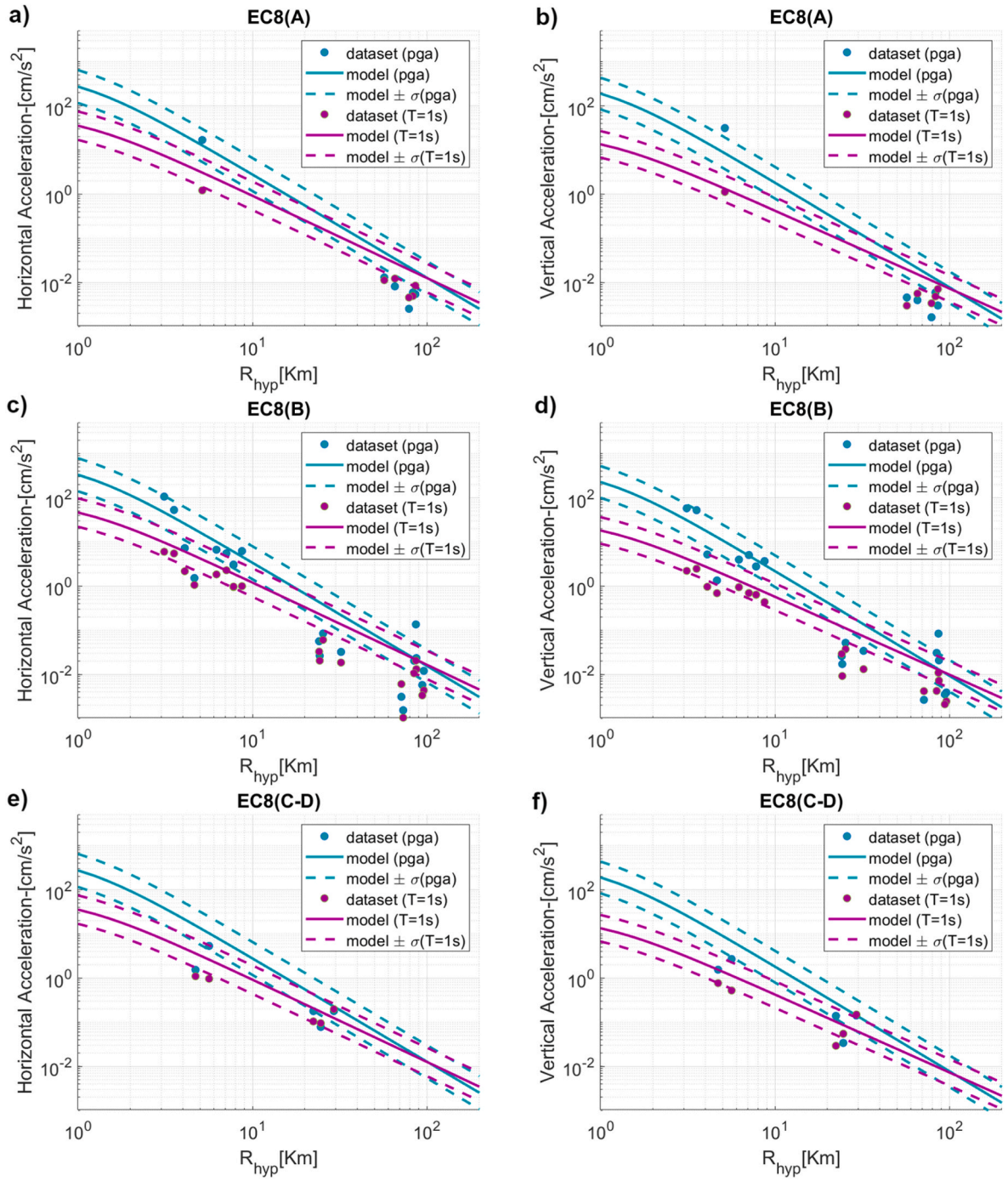

Fig. 6. Comparison between median predictions (±σ) and observations of the M_d 3.5 (M_l 3.7) Phlegrean Fields event for horizontal (left) and vertical (right) components of PGA and SA(1s), as a function of R_{hyp}. Soil category: a, b) EC8-A; c, d) EC8-B; e, f) EC8-C and -D.

uncertainties in the estimation of the location and magnitude of volcanic events with respect to the case of active crustal events. This result is also confirmed by independent modelling of volcanic ground motion by Tusa et al. [12] for Mt. Etna, that also found a total variability larger than 0.4 log10 units at short periods. In both seismotectonic environments, the horizontal sigma is larger than the vertical one at short periods and the peak is shifted to longer periods (T = 0.07s and 0.1s for the vertical and horizontal models, respectively); while at longer periods, we observe the opposite behavior.

4. Check with independent data

An earthquake of magnitude M_d 3.5 was recorded at 3:14 p.m. local time on March 16, 2022 with the epicentre located in the Solfatara area in the Phlegrean Fields (northwest of the city of Naples in Southern Italy) at a depth of about 3 km (Fig. 5). The event is within a swarm that began at 3:12 p.m. local time and consisted of more than 16 earthquakes. The Phlegrean Fields (in Italian Campi Flegrei) are a large volcanic district in the gulf of Pozzuoli, consisting of several craters and volcanic edifices.

About 30 records with epicentral distance less than 100 km are available from the accelerometers installed by RAN network and from accelerometric and broadband instruments installed by INGV networks

(RSN), and 3 stations are located within 3 km from the source: the POZS station (network: IV), located at $R_{epi} = 0.9$ km, recorded a horizontal and vertical PGAs of 0.13 and 0.06 g, respectively; the POZT station (network: IV), located at $R_{epi} = 1.8$ km, PGA = 0.05 g for both horizontal and vertical components; the BAN station (network: IT) with epicentral distance $R_{epi} = 2.6$ km and PGAs<0.01 g. In addition, the CFMN station (network: IV; $R_{epi} = 4.2$ km) recorded non-negligible peak amplitudes with vertical PGA (0.03 g), slightly larger than the horizontal one (0.02 g). These data are useful for three reasons: i) the characteristics of the event allow the model predictions to be compared with such observations that were not used for calibration; ii) the event is shallow and therefore more relevant for engineering applications; and iii) this volcanic district is not represented in the calibration dataset and may allow us to understand how exportable the model is to other volcanic contexts. The intensity measures and the metadata of event and stations are made available as a parametric table in the electronic supplements (Supplement S3), formatted according to the format of the used defined flatfile of ESM [32]. The meanings of the table fields are explained in the user manual, also provided in the supplements.

Fig. 6 shows the attenuation of horizontal and vertical component at PGA and SA (T = 1s) with respect to the hypocentral distance for the median $\pm\boldsymbol{\sigma}$ predictions of the volcanic models and the observed records. In order to obtain the GMM predictions, we use the empirical conversion equation of Tuvè et al. [33], calibrated for Etna volcano-tectonic earthquakes, to derive the local magnitude value M_l 3.7 from the duration magnitude M_d 3.5.

For near source conditions <10 km the model presents a reasonable capability of predicting the event. For longer distances >20 km, the data are more scattered, but, on average, the model slightly overpredicts the observed ground motion.

The acceleration response spectra of the three near source records (BAN, POZS, and POZT) are compared with model predictions for EC8-B class in Fig. 7, both for horizontal and vertical components. Despite there may be some additional uncertainty related the assignment of the EC8 soil category (in the absence of in-situ measurements, inferred from topography), the observed spectra are in good agreement with model predictions, slightly exceeding ± 1 standard deviation in some period ranges: in particular, POZS seems to show a peculiar site effect with an amplification peak at 0.04s.

5. Impact on hazard

Previous studies have shown that the proper assessment of the effects of ground motion in volcanic environments is crucial for hazard estimation (see e.g. Refs. [10,13,41]), however these works focus on the behaviour of the horizontal component of motion, while there are no references to the possible impacts of the vertical volcanic component on site hazard. To address this aim, we here implement some test in the framework of a classical Probabilistic Seismic Hazard Analysis (PSHA [34]), thus adopting a time-independent Poisson model for earthquake occurrence. We use the most up-to-date map of seismogenic sources in Italy - ZS16 [35] - of the area-source model "MA4", which is one of the seismogenic models adopted in the latest version of the Italian seismic hazard map "Modello di Pericolosità Sismica 2019 - MPS19" [36]. This zoning was then used within the R–CRISIS software [37] to perform the present analysis and calculate the Uniform Hazard Spectra (UHS) at the test site for 10% and 2% probability of exceedance in 50 years, corresponding to 475 and 2475 years, respectively. For the latter, we consider the municipality of Zafferana Etnea (Lat: 37.692; Lon: 15.105), which is located in the Italian region of Sicily, and more precisely in source area #49 (Mount Etna), according to ZS16 [35]; see Fig. 8. The Etna region is characterized by earthquakes with hypocentral depths <10 km assigned to the volcanic domain (source area #49) and earthquakes with hypocentral depths ≥10 km assigned to the underlying active crustal source areas (#39, #41, #44, #45, #46, #48) [35]. The analysis implemented here refers to the rates computed for each Source Zone (SZ) within the ZS16 model based on the statistical approach and assuming the maximum magnitude (M_u) with a confidence interval of ±0.2. The distribution of earthquake magnitudes follows the truncated Gutenberg-Richter (GR) model, with the probability density function truncated at both ends. Its cumulative density function related to the moment magnitude is denoted by Λ(M), which is equal to or larger than the magnitude threshold (M_0) and smaller than the first maximum magnitude of the SZ (M_{w1}). The parameters β (the slope) and Λ_0 were derived from the Italian declustered historical earthquake catalogue CPTI15 (Catalogo Parametrico dei Terremoti Italiani version 1.5 [38]; https://emidius.mi.ingv.it/CPTI15-DBMI15/), by adopting the completeness time intervals and the maximum magnitude values. All the parameters of the GR relationships adopted in the calculations for the considered SZs are summarized in Table 2.

The results are shown in Fig. 9 in terms of UHS with reference to the horizontal volcanic and tectonic models, i.e., H-Volcanic vs H-ITA18, respectively, and the vertical ground motion models (V-Volcanic – this study vs V(VH)-ITA18 from VH model by Ramadan et al. [14]).

To better highlight the impact of the model assumed, the analysis is first carried out only in the volcanic zone (area source #49) (Fig. 9a and b) and then activating the hazard contribution of all other nearby areas (Fig. 9 c and d), thus considering volcanic and shallow crustal active sources. In the latter case, the UHS are calculated using the ITA18-V(VH) attenuation model for sources #39, #41, #44, #45, #46, #48 and the proposed volcanic model for shallow events (*depth* < 5 km) in source #49. Therefore, the volcanic model is applied just beyond its validity range (the M_{wmax1} for source zone #49 is 5.6, compared to a maximum magnitude of the calibration dataset of 5.0).

Results in Fig. 9a and b shows a marked difference between the two models, reflecting the already observed trend of Fig. 4, which are also in line with the results provided by Cipriano [40]. In particular, the ordinates of UHS at short periods associated with the volcanic model are

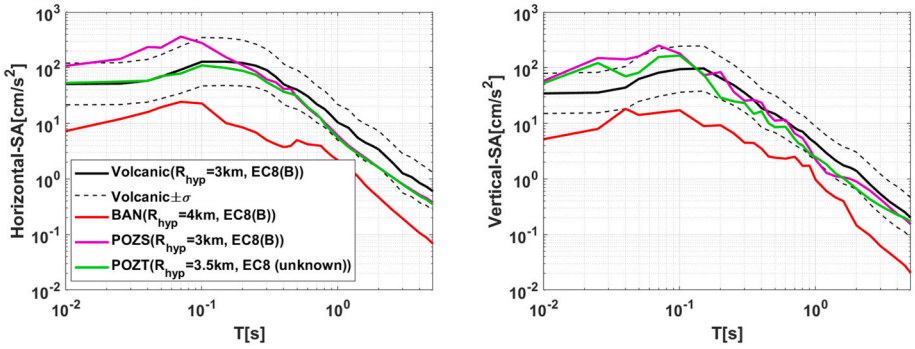

Fig. 7. Comparison between the predicted (±σ) acceleration response spectra (scenario M 3.7, R_{hyp} = 3 km, EC8-B) and those observed during the M_d 3.5 (M_l 3.7) Phlegrean Field earthquake at similar distances for horizontal (left) and vertical (right) components.

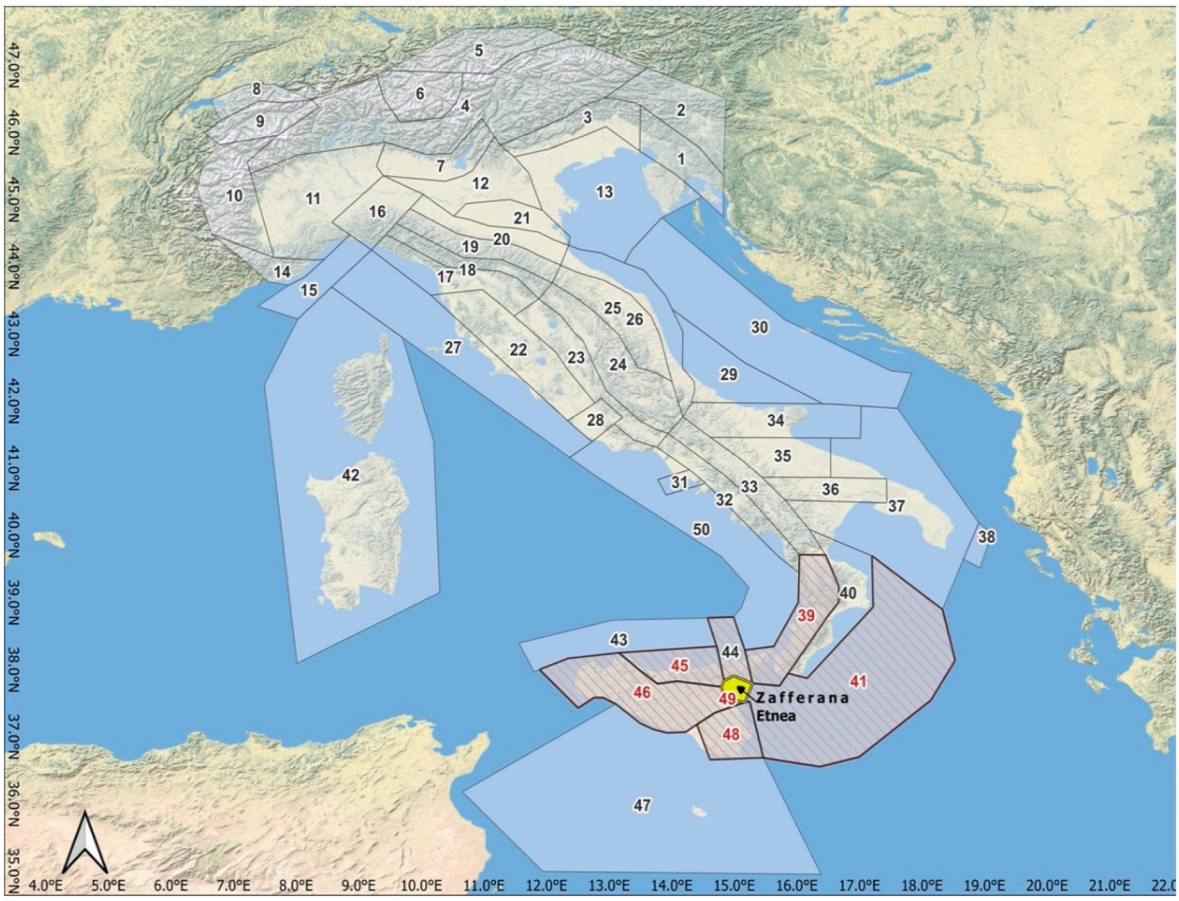

Fig. 8. Map ZS16 (Visini et al. [35]) with polygonal areas representing uniformly distributed seismicity. The SZ9 containing the test site of Zafferana Etnea is highlighted in light green. The other SZs activated for the hazard calculations are evidenced in red mesh.

Table 2
Gutenberg-Richter (GR) parameters, styles of faulting and depth of the SZs adopted in the PSHA of Zafferana Etnea (taken by Ref. [35]).

GR parameters[a]	SZ49	SZ39	SZ41	SZ44	SZ45	SZ46	SZ48	References
b	1.29	0.7	1.2	1.11	0.96	1.2	0.7	Supplement 3 [35]
M_0	3.96	3.96	4.42	4.19	4.19	4.42	4.42	Supplement 3 [35]
$\lambda(M_0)$	0.0412	0.2653	0.0532	0.0927	0.0848	0.0897	0.732	Supplement 3 [35]
β	2.97033	1.61181	2.7631	2.55587	2.21048	2.7631	1.61181	$ln(10) \bullet b$
M_{wmax1}	5.6	7.5	6.7	6.7	6.7	6.7	7.6	Supplement 3 [35]
Style of Faulting	SS	NF	SS	SS	SS	SS	SS	[34]
Hypo1	3	8	–	9	6	10	–	Supplement 1 [35]
Hypo2	–	–	25	–	–	–	22	Supplement 1 [35]
K1	0.011	0.0207	0.011	0.011	0.011	0.011	0.011	[39]

[a] b - Relative ratio of small and large magnitudes; M_0 - Magnitude threshold; $\lambda(M_0)$ - cumulative density function related to the moment magnitude is $\Lambda(M)$; β - Gutenberg-Richter slope; M_{wmax1} - value of maximum magnitude used as Mu in the Truncated GR distibution; Hypo1 - peak of the unimodal (if Hypo2 is empty) distribution that best fits the data (i.e. upper seismogenic layer); K1 - constant of the relationship between the magnitude and the rupture area according to Wells and Coppersmith [39].

significantly lower than those corresponding to the adoption of a tectonic (i.e., shallow active crustal) model, down to about 0.4s for the vertical component. Over longer periods the trend reverses, showing higher UHS estimates for the volcanic model. The pattern is the same at both short and long return periods T_R. In the latter case (2475 ys) the inversion point of the vertical component is shifted toward the left at about 0.25s, thus indicating a more relevant contribution of the volcanic hazard over long periods. This trend is less pronounced when assuming contribution of the other nearby source zones (Fig. 9 c and d), which are capable of producing strong seismicity of a tectonic nature characterized by significantly larger M_{max1}. Actually, we observe the strong influence of the M_{max1} 7.6 of SZ48, which leads to a larger contribution of the spectral content in the long return periods. This is particularly evident for the horizontal components of motion, for which a reversal point between UHS based on ITA18-V(VH) and UHS based on the volcanic model is never observed. On the other hand, for the vertical component, a reversal at 0.3s about is visible. For example, using the ITA18-V(VH) model for the vertical component in the volcanic zone results in an underestimation of the hazard at the site of approximately 4% and 7% at T = 1s, respectively at 475 and 2475 years of return periods.

The hazard disaggregation obtained from R–CRISIS for the Zafferana Etnea site, with the vertical volcanic model proposed here applied to SZ49 and ITA18-V(VH) [14] applied to all neighboring SZs, returns, for the lowest return periods (T_R = 475 years), a dominant scenario identified in higher magnitude intervals (controlled by tectonic events); e.g., 1st mode: Mw 7.11–7.56 and R_{rup} 24–37 km, at both short and long

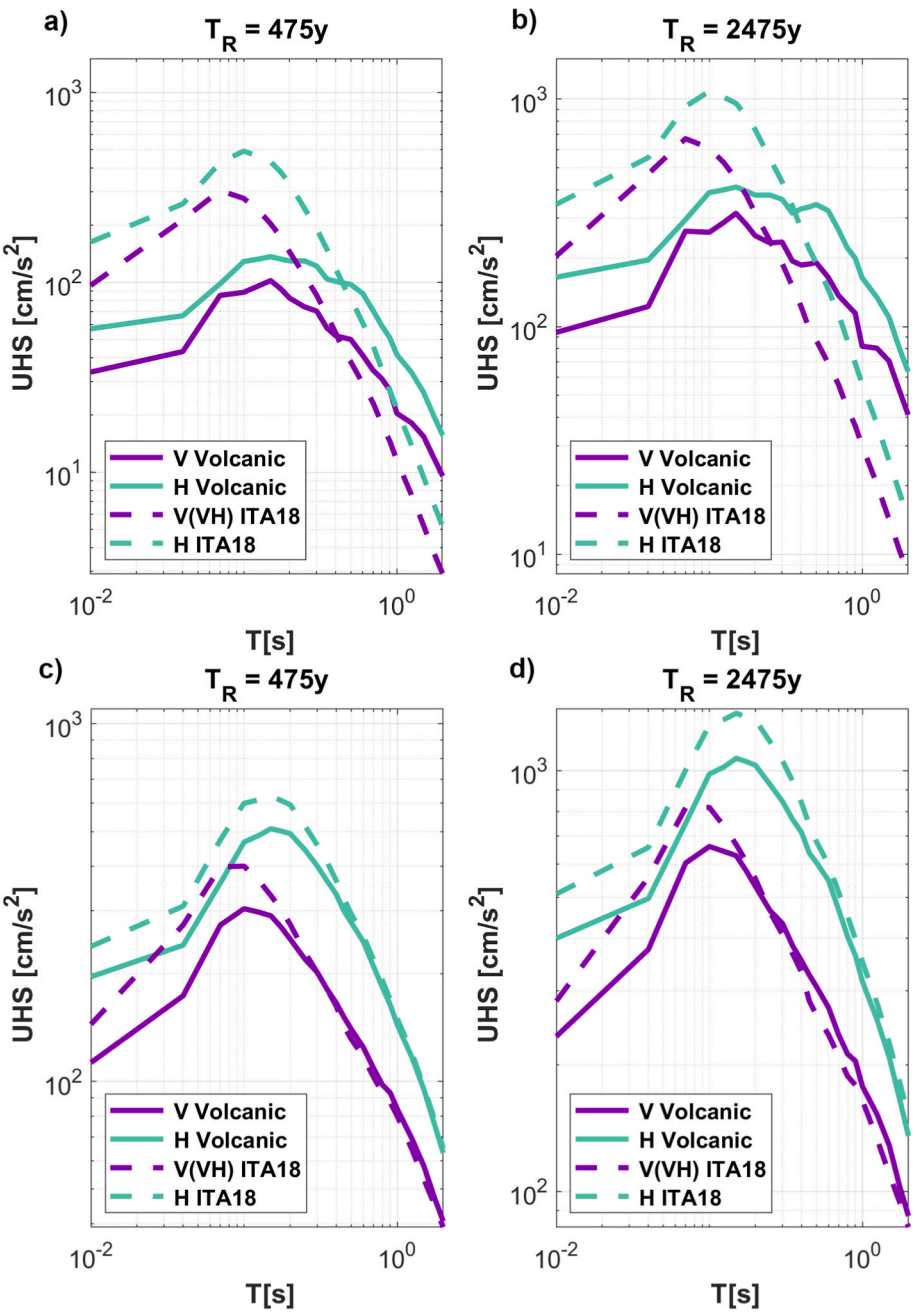

Fig. 9. UHS for rock site ($V_{S,30}$ = 800 m/s) in Zafferana Etnea considering active only the source zone SZ49 at two return periods of 475 years (a) and 2475 years (b) and all the nearby source zones at two return periods of 475 years (c) and 2475 years (d). H volcanic is the model by Lanzano and Luzi [1]; V volcanic is the model presented here; H ITA18 is the model by Lanzano et al. [27]; V ITA18 is the model by Ramadan et al. [14]. The ITA18 predictions are provided for strike-slip earthquakes.

periods. In contrast, at T_R = 2475 years and long periods, a bimodal scenario results from both tectonic and volcanic seismicity. For example, at SA(1s) the dominant scenario shifts to lower magnitude intervals (controlled mainly by volcanic events); e.g. SA(1s) 1st mode: Mw 5.33–5.78 and R_{rup} 0–12 km; 2nd mode: 7.11–7.56 and R_{rup} 24–37 km.

Fig. 10 shows the UHS ratios (i.e., the ratio of the spectral ordinates V/H) related to SZ49. Here the ordinates associated with ITA18 assume a peak at 0.04s that is greater than the conventional 2/3 assumed in the standard codes for the vertical/horizontal ratio, in agreement with the findings by Ramadan et al. [14]; this trend tends to decrease as structural periods increase, with an absolute minimum near 0.45 at T = 0.2 s. On the other hand, the spectral ratios for the volcanic model assume lower values than the tectonic case at short periods, although there is a significant increase for vibration periods greater than 0.06 s (reverse point). In this case, the underestimation of seismic hazard in the volcanic zone due to the adoption of the tectonic model is about 27% at 475 yrs and 36% at 2475 yrs, on average, in the period range 0.05–0.6s. Note that these curves show a reversal trend with respect to the return period T_R; i.e. the ratio is higher for lower T_R (475yrs) in the case of short and intermediate periods for the volcanic model, then reverses over longer periods.

6. Conclusions

The seismic risk in volcanic areas in Italy is relevant because some of the most dangerous active volcanoes (the Mount Etna, the Mount Vesuvius and the Phlegrean fields) are located near densely populated areas, such as the cities of Naples and Catania, where strategic infrastructure and hazardous plants are also installed. This consideration makes it necessary to consider the seismic hazard induced by volcanic activity along with that related to active crustal events for the definition of the overall hazard to the site, either by deterministic or probabilistic approach.

However, engineering-relevant seismic events of volcanic origin (M

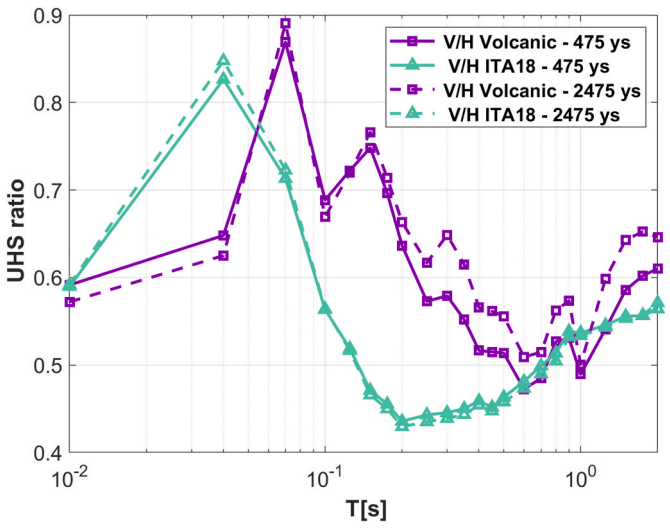

Fig. 10. UHS ratios for the rock site ($V_{S,30}$ = 800 m/s) at Zafferana Etnea in SZ49: comparison between volcanic model and ITA18 at two return periods of 475 and 2475 years.

> 3.5) have a lower frequency of occurrence than earthquakes of tectonic origin in Italy. This has made it more difficult to study seismic motion in volcanic areas and to calibrate prediction models on a fully empirical basis that can be used in seismic hazard analyses. Despite this limitation, the recent exceptional growth of seismic monitoring in Italy allowed the collection of several observations for the latest events of moderate magnitude in different volcanic districts (the Mount Etna 2018 M_W 4.9, the Ischia Island 2017 M_W 3.9 and the Phlegrean Fields 2022 M_d 3.5), and particularly in near-source conditions. This allowed us to observe that very close to the epicenter (R_{epi}<3 km), the peak acceleration values and ordinates of the short-period spectrum can be relevant even for small-to-medium earthquakes (PGA>0.1 g for M = 3.5).

The new data made it possible to fruitfully update empirical models for the prediction of volcanic events, like those proposed by Lanzano and Luzi [1] and Tusa et al. [12], extending the validity of the GMMs to magnitude 5.0. The result presented here is a further step forward in the definition of seismic motion in volcanic areas in Italy, updating the predictions of Lanzano and Luzi [1] with the introduction of the magnitude-dependent attenuation in the functional form and extending the GMMs to vertical components of the motion for PGA, PGV and the amplitudes of the acceleration spectra, 5% damping, in the period interval T = 0.025–5s. In fact, the study of near-source recordings of tectonic events has shown that the vertical component of motion could be significantly higher than the horizontal component [14], with significant implications in the seismic design of structures sensitive to vertical actions. Empirical modelling of the vertical component of seismic motion of volcanic earthquakes has shown that: (i) the characteristics of horizontal and vertical seismic motion are the same (significant amplitudes in near-source, rapid attenuation with distance, peak frequency content shifted to lower frequencies); (ii) surface and deep volcanic earthquakes have different characteristics, and surface earthquakes, which are most relevant for hazard estimation, are markedly different from tectonic earthquakes; (iii) vertical motion seems to have lower, or at most equal, amplitudes than horizontal motion, even near the source.

The comparison with the independent event that occurred on March 16, 2022 in the Phlegrean Fields (Md 3.5) showed that the proposed model reasonably predicts the observed ground motion for both the horizontal and vertical components, slightly overestimating the attenuation with distance.

Finally, the example application of the proposed model in the context of a PSHA to a site near the volcano Etna revealed that the UHS of the vertical component shows a dominant trend at long periods (greater than 0.3s) with respect to the tectonic model. This behavior contrasts with that observed for the horizontal components, for which the tectonic seismicity tend to control the hazard at all the return periods investigated. We find that using the ITA18 model for the vertical component produces hazard spectra that attenuates more rapidly on long periods compared to the actual propagation properties in the volcanic area, resulting in underestimation of the vertical-to-horizontal ratio of the UHS estimates in the period range 0.05–0.6s.

Another relevant finding is that the effects of vertical volcanic earthquakes tend to become dominant, compared to the hazard contribution of the large regional tectonic structures, at long exposure periods (475 and 2475 years), which is also in contrast to what has been previously observed for the horizontal components (i.e. the highest effects of volcanic earthquakes have been shown at short periods ~5–30 years, e.g. Peruzza et al. [10]). These findings suggest the need to consider volcanic domain-specific models in hazard applications, in order to adequately account for the peculiar behavior of ground motion in these contexts.

Further development will aim testing the model in other volcanic settings, including those outside Italy, such as Hawaii and the Azores, which have fairly dense monitoring networks. The ambitious long-term goal could be to explore the possibility of calibrating a global volcanic model by introducing the specificities of each volcanic district through random effects, as is now routinely done in the calibration of non-ergodic models.

Supplementary Materials: Supplement S1: collection of additional plots; Supplement S2: table of coefficients and standard deviations of the GMM proposed here for horizontal and vertical components; Supplement S3: parametric table of the intensity measures and the metadata of event and stations of the Phlegrean fields March 16, 2022, M_d 3.5, earthquake (ITACA ID: INT-20220316_0000131).

Author contributions

All authors participated in the preparation and submission stages of the manuscript.

Funding

This work was partially funded by the SIGMA2 consortium (EDF, CEA, PG&E, SwissNuclear, Orano, CEZ, CRIEPI) 2017–2021 as a tool to support the analysis of the strong motion of very shallow event. This study has been also partially developed within the research programs INGV-ReLUIS (Rete dei Laboratori Universitari di Insegneria Sismica) in the framework of the DPC-ReLUIS Agreement 2022–2024 ″COntributi Normativi Progetto Azione Sismica (CONPAS)" WP18 coordinated by Prof. Roberto Paolucci, funded by the Presidenza del Consiglio dei Ministri - Dipartimento della Protezione Civile (DPC), Italy.

Declaration of competing interest

The authors declare no conflict of interest.

Data availability

Data are attached as electronic supplements or are available through public links

Acknowledgments

The authors wish to thank the INGV (Istituto Nazionale di Geofisica e Vulcanologia) ESM/ITACA Working Group in Milan, for their effort in the development of the strong motion databases the constitute the reference data of our analysis. Prof. Chiara Smerzini (Politecnico di Milano), Dott. Paola Traversa (Électricité de France) and Arianna

Cipriano (SOIL Engineering Spa) are also acknowledged for their scientific support and encouragement in this research. The authors would also like to thank their INGV-Milan colleague Paolo Augliera for helpful suggestions during the revision phase of the manuscript. Finally, we sincerely thank the reviewers for the useful comments.

Appendix A. Supplementary data

Supplementary data to this article can be found online at https://doi.org/10.1016/j.soildyn.2023.108228.

References

[1] Lanzano G, Luzi L. A ground motion model for volcanic areas in Italy. Bull Earthq Eng 2020;18(1):57–76.
[2] Locati M, Camassi R, Rovida A, Ercolani E, Bernardini F, Castelli V, Caracciolo CH, Tertulliani A, Rossi A, Azzaro R, D'Amico S, Conte S, Rocchetti E, Antonucci A. Database Macrosismico Italiano (DBMI15), versione 4.0. Istituto Na-zionale di Geofisica e Vulcanologia (INGV). https://doi.org/10.13127/dbmi/dbmi15.4; 2022.
[3] Pitt AM, Hill DP. Long-period earthquakes in the long valley caldera region, eastern California. Geophys Res Lett 1994;21(16):1679–82.
[4] Tusa G, Langer H. Prediction of ground motion parameters for the volcanic area of Mount Etna. J Seismol 2015;20(1):1–42.
[5] Giampiccolo E, Cocina O, De Gori P, et al. Dyke intrusion and stress-induced collapse of volcano flanks: the example of the 2018 event at Mt. Etna (Sicily, Italy). Sci Rep 2020;10:6373.
[6] Vanorio T, Virieux J, Capuano P, Russo G. Three-dimensional seismic tomography from P wave and S wave microearthquake travel times and rock physics characterization of the Campi Flegrei Caldera. J Geophys Res Solid Earth 2005;110 (B3).
[7] Capuano P, De Matteis R, Russo G. The structural setting of the Ischia Island Caldera (Italy): first evidence from seismic and gravity data. Bull Volcanol 2015; 77:1–10.
[8] Azzaro R, Barbano MS, D'Amico S, Tuvè T. The attenuation of seismic intensity on the Etna region and comparison with other Italian volcanic districts. Ann Geophys 2006;49(4/5):1003–20.
[9] Iervolino I Editoriale. Il moto al suolo nel terremoto di Viagrande (CT). Progettazione Sismica; 2019 (in Italian).
[10] Peruzza L, Azzaro R, Gee R, D'Amico S, Langer H, Lombardo G, Pace B, Pagani M, Panzera F, Ordaz M, Suarez ML, Tusa G. When probabilistic seismic hazard climbs volcanoes: the Mt. Etna case, Italy—part 2: computational imple-mentation and first results. Nat Hazards Earth Syst Sci 2017;17:1999–2015.
[11] Meletti C, et al. The new Italian seismic hazard model (MPS19). Ann Geophys 2021;64(1).
[12] Tusa G, Langer H, Azzaro R. Localizing ground-motion models in volcanic terranes: shallow events at Mt. Etna, Italy, revisited. Bull Seismol Soc Am 2020;110(6): 2843–61.
[13] Azzaro R, Barberi G, D'Amico S, Pace B, Peruzza L, Tuvè T. When probabilistic seismic hazard climbs volcanoes: the Mt Etna case, Italy—Part 1: model components for sources parametrization. Nat Hazards Earth Syst Sci 2017;17: 1981–98.
[14] Ramadan F, Smerzini C, Lanzano G, Pacor F. A ground motion model for vertical-to-horizontal response spectral ratios for shallow crustal earthquakes in Italy. Earthq Eng Struct Dynam 2021;50(15):4121–414.
[15] Luzi L, Lanzano G, Felicetta C, D'Amico MC, Russo E, Sgobba S, Pacor F, ORFEUS Working Group. Engineering strong motion database (ESM) (version 2.0). Istituto Nazionale di Geofisica e Vulcanologia (INGV); 2020. https://doi.org/10.13127/ESM.2.
[16] Russo E, Felicetta C, D'Amico M, Sgobba S, Lanzano G, Mascandola C, Pacor F, Luzi L. Italian Accelerometric Archive v3.2 - Istituto Nazionale di Geofisica e Vulcanologia. Dipartimento della Protezione Civile Nazionale 2022. https://doi.org/10.13127/itaca.3.2.
[17] Presidency of Council of Ministers - Civil Protection Department. Italian strong motion network [data set]. Interna-tional Federation of Digital Seismograph Networks; 1972. https://doi.org/10.7914/SN/IT.
[18] INGV Seismological Data Centre. Rete Sismica Nazionale (RSN). Istituto Nazionale di Geofisica e Vulcanologia (INGV), Italy. 2006. https://doi.org/10.13127/SD/X0FXnH7QfY.
[19] MedNet Project Partner Institutions. Mediterranean Very Broadband Seismographic Network (MedNet). Istituto Nazionale di Geofisica e Vulcanologia (INGV). 1990. https://doi.org/10.13127/SD/fBBBtDtd6q.
[20] Puglia R, Russo E, Luzi L, D'Amico M, Felicetta C, Pacor F, Lanzano G. Strong-motion processing service: a tool to ac-cess and analyse earthquakes strong-motion waveforms. Bull Earthq Eng 2018;16(7):2641–51.
[21] Paolucci R, Pacor F, Puglia R, Ameri G, Cauzzi C, Massa M. Record processing in ITACA, the new Italian strong-motion database. In: Akkar S, Gülkan P, van Eck T, editors. Earthquake data in engineering seismology—predictive models, data management and networks. Geotechnical, geological, and earthquake engineering, vol. 14. Dordrecht: Springer; 2011. 978-94-007-0151-9 (printed version)978-94-007-0152-6 (E-book version).
[22] Cen. EuroCode 8: design of structures for earthquake resistance—part 1: general rules, seismic actions and rules for buildings. Bruxelles: European Committee for Standardization; 2004.
[23] Wald DJ, Allen TI. Topographic slope as a proxy for seismic site conditions and amplification. Bull Seismol Soc Am 2007;97(5):1379–95.
[24] Gasperini P, Lolli B, Vannucci G. Empirical calibration of local magnitude data sets versus moment magnitude in Italy. Bull Seismol Soc Am 2013;103(4):2227–46. https://doi.org/10.1785/0120120356.
[25] Al Atik L, Abrahamson N, Bommer JJ, Scherbaum F, Cotton F, Kuehn N. The variability of ground-motion prediction models and its components. Seismol Res Lett 2010;81(5):794–801.
[26] Bates D, Mächler M, Bolker B, Walker S. Fitting linear mixed-effects models using lme4. J Stat Software 2015;67(1):1–48.
[27] Lanzano G, Luzi L, Pacor F, Felicetta C, Puglia R, Sgobba S, D'Amico M. A revised ground motion prediction model for shallow crustal earthquakes in Italy. Bull Seismol Soc Am 2019;109(2):525–40.
[28] Bessason B, Kaynia AM. Site amplification in lava rock on soft sediments. Soil Dynam Earthq Eng 2002;22(7):525–40.
[29] Moscatelli M, et al. Physical stratigraphy and geotechnical properties controlling the local seismic response in explosive volcanic settings: the Stracciacappa maar (central Italy). Bull Eng Geol Environ 2021;80:179–99.
[30] Rahpeyma S, Halldorsson B, Olivera C, Green RA, Jonsson S. Detailed site effect estimation in the presence of strong velocity reversals within a small-aperture strong-motion array in Iceland. Soil Dynam Earthq Eng 2016;89:136–51.
[31] Rahpeyma S, Halldorsson B, Hrafnkelsson B, Darzi A. Frequency-dependent site amplification functions for key geological units in Iceland from a Bayesian hierarchical model for earthquake strong-motions. Soil Dynam Earthq Eng 2023; 168:107823.
[32] Lanzano G, Sgobba S, Luzi L, Puglia R, Pacor F, Felicetta C, D'Amico M, Cotton F, Bindi D. The pan-European Engineering Strong Motion (ESM) flatfile: compilation criteria and data statistics. Bull Earthq Eng 2019;17(2):561–82.
[33] Tuvè T, D'Amico S, Giampiccolo E. A new MD-ML relationship for Mt. Etna earthquakes (Italy). Ann Geophys 2015;58(6):1–8.
[34] Cornell CA. Engineering seismic risk analysis. Bulletin of the Seismological Society of America; 1968.
[35] Visini F, Meletti C, Rovida A, D'Amico V, Pace B, Pondrelli S. Updated area-source seismogenic model for seismic hazard of Italy. Nat Hazards Earth Syst Sci 2022: 2807–27.
[36] Ordaz M, Salgado-Gálvez MA. R-CRISIS v20 validation and verification document. In: ERN technical report., Mexico City, Mexico.; 2020.
[37] Meletti C, Marzocchi W, D'Amico V, Lanzano G, Luzi L, Martinelli F, Pace B, Rovida A, Taroni M, Visini F. And the MPS19 working Group: the new Italian seismic hazard model (MPS19). Ann Geophys 2021;64(1). https://doi.org/10.4401/ag-8579.
[38] Rovida A, Locati M, Camassi R, Lolli B, Gasperini P. CPTI15, the 2015 version of the parametric catalogue of Italian earthquakes. Istituto Nazionale di Geofisica e Vulcanologia; 2016.
[39] Wells DL, Coppersmith KJ. New empirical relationships among magnitude, rupture length, rupture width, rupture area and surface displacement. Bull Seismol Soc Am 1994;84.
[40] Cipriano A. Thesis: impact of Italian ground motion models in seismic hazard assessment: case studies in near-source region and volcanic context. In: Politecnico di Milano (Italy); 2022. http://hdl.handle.net/10589/197115.
[41] Azzaro R, D'Amico S, Peruzza L, Tuvè T. Probabilistic seismic hazard at Mt. Etna (Italy): the contribution of local 20 fault activity in mid-term assessment. J Volcanol Geoth Res 2013;251:158–69.